NUMERICAL ANALYSIS OF INTERGRANULAR DAMAGE AND FRACTURE BEHAVIOR OF BRITTLE CONTINUA WITH STOCHASTIC GRAIN BOUNDARIES

J.R. Li, Z.J. Zheng and J.L. Yu*
CAS Key Laboratory of Mechanical Behavior and Design of Materials
University of Science and Technology of China, Hefei 230026, China

ABSTRACT

Intergranular fracture is a common failure mode in continua. Weak interfaces or grain boundaries are easily damaged and cracked under loading. Thereby, the fraction and distribution of the weak interfaces plays an important role in the intergranular fracture of brittle solids.

In this paper, we study the influence of weak interface fraction and connectivity on the intergranular failure of brittle solids. A two-dimensional stochastic finite element method (SFEM) is used to investigate the stochastic intergranular damage and failure. The grain interface is treated as a cohesive zone. The strength and toughness of the isolated interface is random. First, the strength distribution of the interfaces is treated to follow a normal distribution. The failure process and the fracture performance of the solids are investigated. Then, the interfaces are divided into two groups: one is weak interface and the other is strong interface with specific interface properties, respectively. The influence of the weak interface fraction and connectivity on the fracture behaviors is analyzed and discussed. It is found that the fracture energy do not decrease monotonously with the increase in the weak interface fraction. In a certain stage some toughening effect with increasing weak interfaces exists. On the other hand, weak interface connectivity statistically has a little influence on the intergranular failure of brittle solids.

1 INTRODUCTION

Intergranular fracture is a common failure mode in continua. Weak interfaces or grain boundaries are easily damaged and cracked under loading. Thereby, the fraction and distribution of the weak interfaces plays an important role in the intergranular fracture of brittle solids. A review of the mathematical and microstructural foundations of the size effect on the average tensile strength and statistics of fracture in random materials was presented by Duxbury et al [1].

For metallic polycrystals, it was found that the grain boundaries could be described into two groups: special grain boundaries with higher strength and random grain boundaries with lower strength (Watanabe [2]). Optimization of the grain boundary character distribution (GBCD) and the grain boundary connectivity can improve the performance in both structural and functional polycrystalline materials (Watanabe [3,4]).

Carmeliet and Hens [5] employed nonlocal continuum damage mechanics and random field theory to model the stochastic damage behavior of a strain-softening material with random field properties. Zavattieri and Espinosa [6] treated the grain interface as a cohesive zone and simulated the microcrack initiation, propagation and coalescence, as well as crack interaction and branching.

In this paper, a two-dimensional stochastic finite element method (SFEM) is employed to investigate the damage process and the fracture behavior of brittle continua. A cohesive zone model is used to represent the grain interface. The strength and toughness of the isolated interface

* Corresponding author. Tel.: +86-551-3603793; fax: +86-551-3606459
E-mail address: jlyu@ustc.edu.cn (J.L. Yu)

is random. The strength distribution of the interfaces is firstly treated to follow a normal distribution. Then, for simplicity, the interfaces are divided into two groups, i.e. weak interfaces and strong interfaces. The influences of weak interface fraction and its connectivity on the fracture behaviors of brittle continua are investigated.

2 COMPUTATIONAL MODEL

The influences of the weak interface fraction and the weak interface connectivity on the intergranular fracture are investigated using a polycrystalline model, which is presented in Fig. 1. The specimen is modeled as a two-dimensional strip with a width of 15.0 mm and a length of 34.64 mm. It includes 175 full grains with 12 elements (type CPS3) and 50 half grains with 6 elements. The material data of concrete are taken as an example in the model, for concrete is a typical brittle material with granular structure. The concrete grain is regarded as a linearly elastic material with the mean Young's modulus of 25 GPa, the Possion's ratio of 0.15 and the density of 2400 kg/m^3. To simulate the quasi-static load, a constant velocity of 1 mm/s in the horizontal direction was applied to the right edge of the strip, while the left edge was fixed in the horizontal direction and the middle point of the left edge was fixed in the vertical direction.

A multi-body contact-interface algorithm describing the kinematics at the grain boundaries is used to simulate crack initiation and propagation. A cohesive zone model called "spot welds" in the ABAQUS code [7] is employed to simulate the intergranular cracking. The critical condition of failure is detected according to the linear force-displacement relationships. The failure initiation and post-failure behavior of a spot weld is described by

$$\left(\frac{\max(\sigma^n,0)}{\sigma_{cr}^n}\right)^2+\left(\frac{\sigma^s}{\sigma_{cr}^s}\right)^2\le 1.0-\frac{G^n}{G_f^n}-\frac{G^s}{G_f^s}, \tag{1}$$

where σ^n and σ^s are the normal stress and shear stress of the interface, σ_{cr}^n and σ_{cr}^s the tensile and shear strengths, respectively, G^n and G^s the normal and shear energies of the interface, $G_f^n=\sigma_{cr}^n u_f^n/2d$ and $G_f^s=\sigma_{cr}^s u_f^s/2d$ the breakage energies in Mode I and Mode II, u_f^n and u_f^s the normal and shear breakage displacements of the interface, respectively, d the coarse grain size. In this simulation, it is assumed that the breakage energies of Mode I and Mode II are proportional to the tensile and shear strengths, i.e. $G_f^I/G_f^{II}=\sigma_{cr}^n/\sigma_{cr}^s$, and this ratio is taken as 2 for each interface. When the tensile strength σ_{cr}^n is taken as 4MPa, the Mode I fracture energy G_f^I is given as 0.0577MPa, i.e. $u_f^n=u_f^s=0.05$mm.

Stochastic material properties of isolated grains are endued, which follow a normal distribution with the mean Young's modulus of 25GPa and the standard deviation of 1GPa. Mechanical properties of isolated interfaces are also randomly endued.

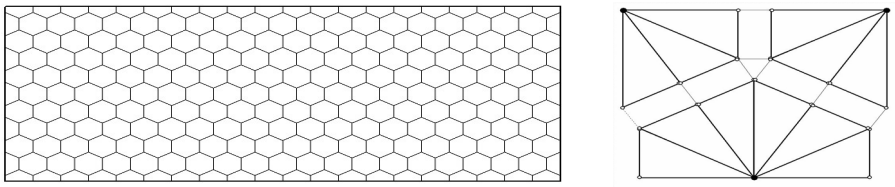

Figure 1: The polycrystal model: (a) a strip of 15.0 mm x 34.64 mm, and (b) its interface elements in grain boundaries.

First, the strengths of interfaces are treated to follow a normal distribution with the mean strength 4MPa and its standard deviation s =0.4, 0.6, 0.8, 1.0MPa, respectively. As the standard deviation of the interfacial strength increases, the weak interface number trends to increase. 50 sets of different random interface distributions for the model are calculated. The qualitative analyses of the influence of the weak interface number on the intergranular fracture are investigated.

To study quantitatively the influence of the weak interface number N_w and the weak interface connectivity on the intergranular fracture, for simplicity, the interfaces are treated into two groups, i.e. strong interfaces with σ_{cr}^{n} = 4MPa and σ_{cr}^{s} = 2MPa and weak interfaces with σ_{cr}^{n} = 2MPa and σ_{cr}^{s} = 1MPa. The total interface number in the model is 614. Some interfaces are randomly selected as weak interfaces, and the others are treated as strong interfaces. 50 sets of different random interface distributions are calculated. Each set consists of 10 samples with the number of weak interfaces increasing from 30 to 300 by an interval of 30 (denoted as N_w= 30:30:300), generated from a random number list.

3 RESULTS AND DISCUSSION

The fracture energy per unit volume is calculated by

$$G_f = \int_0^{\varepsilon_f} \sigma d\varepsilon \,, \tag{2}$$

where ε_f is the fracture strain of the strip. Fig. 2 shows the variations of the statistic fracture energy and fracture strain with the standard deviation of the interfacial strength. It indicates that with the increase in the standard deviation of the interfacial strength the statistic fracture energy and fracture strain decrease. Fig. 3 shows the nominal stress-strain curves of typical samples of different standard deviations but in the same random interface list. Fig. 4 shows the corresponding final fractured interfaces. It seems that the final failure paths are almost the same though their mechanic responses are different. Thereby, it is reasonable to divide interfaces into two groups: weak interfaces and strong interfaces.

For simplicity, the interfaces are divided into two groups: one is weak interface and the other is strong with specific interface properties, respectively. Fig. 5 shows the variations of the fracture energy and fracture strain of a typical set of samples with the increase in the weak interface number. The two curves do not decrease monotonously with the increase in weak interface number. At the initial stage, the weak interfaces strongly affect the failure path. With an increase in the weak interface fraction, fracture performance trends to steadily decrease for the main failure path is formed. Other failure paths appear with further increase in the weak interface fraction, and the fracture energy and fracture strain appear to increase and decrease in several stages. Finally, when the weak interfaces are largely distributed, the fracture energy is much low and changes very little with the variation of the weak interface fraction.

To analyze the toughening effect with the increasing weak interface fraction in detail, two typical models, denoted here as model A with 110 weak interfaces and model B with added 37 weak interfaces on model A, are shown in Fig. 6. The nominal stress-strain curves of models A and B are shown in Fig. 7. It is evident that the strength of model B is lower than that of model A, but the fracture energy and fracture strain of model B are rather larger than those of model A. Fig. 8 shows the final fracture interfaces of models A and B.

The results of the total 50 sets of samples with N_w= 30:30:300 are statistically analyzed. The variations of the statistic fracture energy and fracture strain with the weak interface fraction and their mean square deviations are shown in Fig. 9. It transpires that the fracture energy and fracture strain do not decrease monotonously with the increase in the weak interface fraction. A stage with

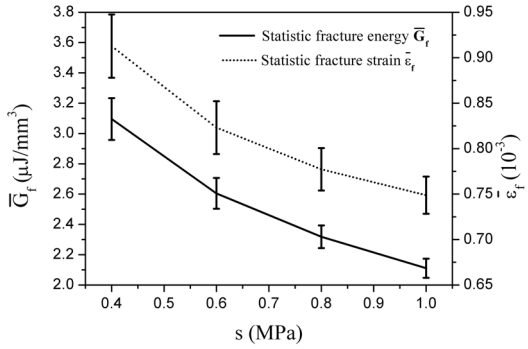

Figure 2: Variations of the statistic fracture energy and fracture strain with the standard deviation of the interfacial strength.

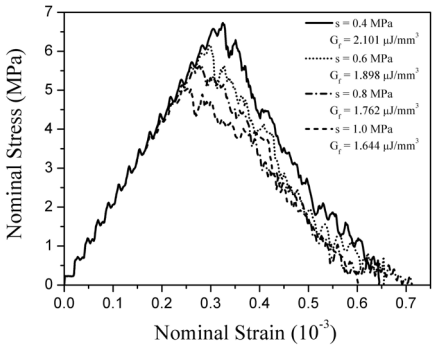

Figure 3: The nominal stress-strain curves of different standard deviations of the interfacial strength for a same random sample list.

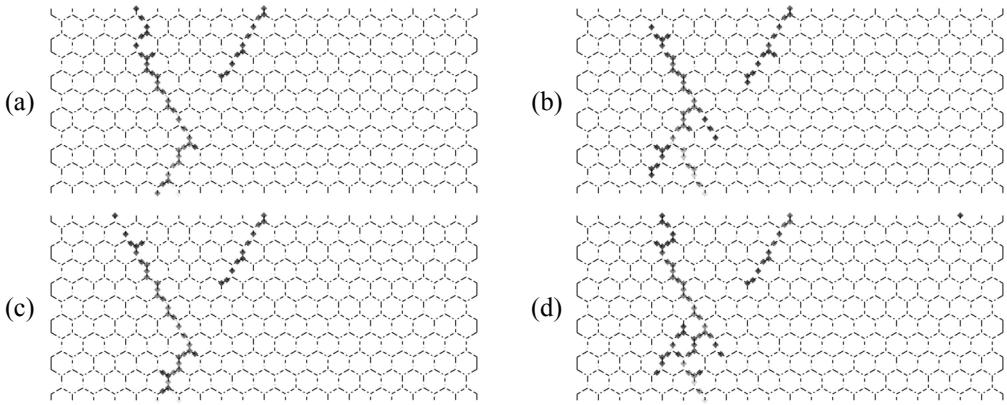

Figure 4: Final fractured interfaces for an identical random sample list with different standard deviations of the interfacial strength: (a) s = 0.4 MPa, (b) s = 0.6 MPa, (c) s = 0.8 MPa, and (d) s = 1.0 MPa.

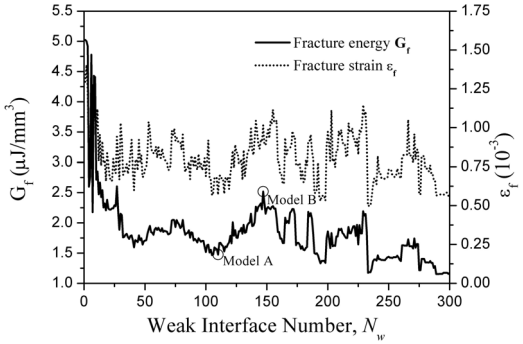

Figure 5: Variations of fracture energy and fracture strain with the weak interface number.

certain increase of fracture energy exists, indicating some toughening effect with the increasing weak interface fraction. The influence of the weak interface connectivity, described by the weak interface correlation length L_w defined as the ratio of the weak interface number to the independent weak interface number, on the fracture energy is also investigated.

With the increase in the weak interface fraction, the weak interface correlation length increases almost in an exponential law. The statistical result can be fitted by

$$L_w = 0.8093 + 0.2455 * \exp(f_w / 0.1846) , \quad (3)$$

where f_w is the weak interface fraction. The statistical fracture energy trends to decrease while the weak interface correlation length increases. Their relation can be fitted by an exponential law,

$$G_f = 1.426 + 4.961 * \exp(-L_w / 0.6998) \ \ (\mu J/mm^3) , \quad (4)$$

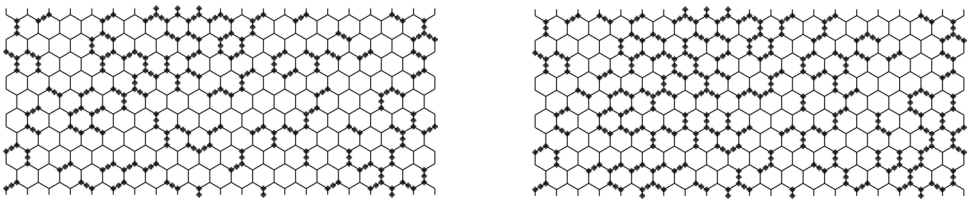

(a) (b)

Figure 6: Sequent weak interface distributions with (a) 110 weak interfaces, model A, and (b) 147 weak interfaces, model B.

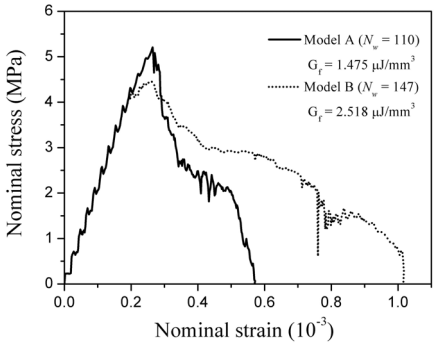

Figure 7: The nominal stress-strain curves of models A and B.

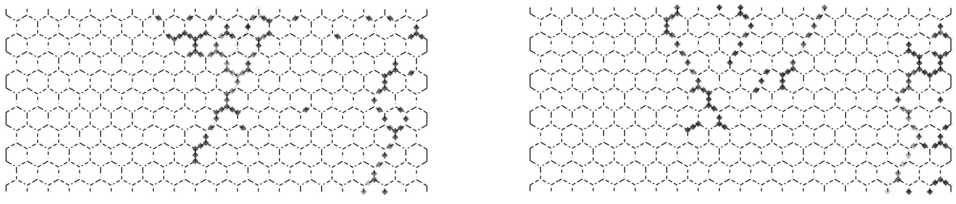

(a) (b)

Figure 8: Final fractured interfaces in (a) model A with 110 weak interfaces and (b) model B with 147 weak interfaces.

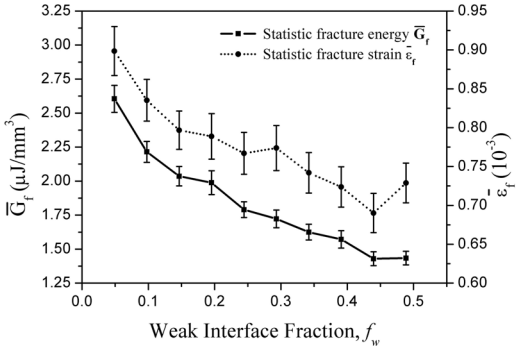

Figure 9: Variations of statistic fracture energy and statistic fracture strain with the weak interface fraction.

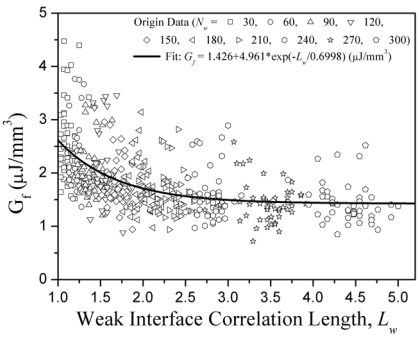

Figure 10: Variation of the fracture energy with the weak interface connectivity.

as shown in Fig. 10. It indicates that the weak interface connectivity do have some influence on the fracture performance.

4 CONCLUSION

In this paper, the damage process and the fracture behavior of brittle continua are simulated using the stochastic finite element method. The influence of the weak interface fraction and its connectivity on the fracture performance is investigated. The results show that weak interfaces significantly affect the material performance. However, the fracture energy and fracture strain do not decrease monotonously with the increasing weak interface fraction. Both the individual and statistical results indicate certain toughening effect, i.e., an increase in weak interfaces in some range will enhance the fracture performance. Increase in the weak interface connectivity may weaken the fracture performance, but this effect is not very significantly comparing with the effect of the weak interface fraction.

REFERENCE

[1] Duxbury PM, Kim SG, Leath PL. Size effect and statistics of fracture in random materials. Materials Science and Engineering, A 176, 25-31, 1994.

[2] Watanabe T. An approach to grain boundary design for strong and ductile polycrystals. Res Mechanica, 11 (1), 47-84, 1984.

[3] Watanabe T. The impact of grain boundary character distribution on fracture in polycrystals. Materials Science and Engineering, A 176, 39-49, 1994.

[4] Watanabe T. Tsuerekawa S. The control of brittleness and development of desirable mechanical properties in polycrystalline systems by grain boundary engineering. Acta Materialia, 47 (15), 4171-4185, 1999.

[5] Carmeliet J, Hens H. Probabilistic nonlocal damage model for continua with random field properties. Journal of Engineering, 120 (10), 2013-2027, 1994.

[6] Zavattieri PD, Espinosa HD. Grain level analysis of crack initiation and propagation in brittle materials. Acta Materialia, 49 (20), 4291-4311, 2001.

[7] ABAQUS, Version 5.8. Hibbitt, Karlsson and Sorensen, Inc., Pawtucket, RI, 1998.